Journal of Nuclear Materials 385 (2009) 11–14

Contents lists available at ScienceDirect

Journal of Nuclear Materials

journal homepage: www.elsevier.com/locate/jnucmat

Crystal structure and physical properties of $PuPd_5Al_2$

J.-C. Griveau *, K. Gofryk, E. Colineau, J. Rebizant

European Commission, Joint Research Centre, Institute for Transuranium Elements, Postfach 2340, 76125 Karlsruhe, Germany

ARTICLE INFO

PACS:
71.20.Lp
61.10.Eq
75.50.Ee

ABSTRACT

We report on the crystallographic aspects and the basic properties of the plutonium based compound $PuPd_5Al_2$. This material is antiferromagnetic at $T_N = 5.6$ K and does not present any hint of superconductivity down to 2 K. This material crystallizes in the $ZrNi_2Al_5$-type of structure with lattice parameters: $a = 4.1302$ Å and $c = 14.8428$ Å. The magnetization, heat capacity and electrical resistivity measurements indicate clearly antiferromagnetic order at $T_N = 5.6$ K. This material is compared to the structurally related cerium based material $CePd_5Al_2$ presenting superconductivity induced by pressure.

1. Introduction

Superconductivity has been reported recently in $NpPd_5Al_2$ [1], a neptunium based intermetallic compound. It has been found that this material displays d-wave superconductivity ($T_c = 4.9$ K) and heavy-fermion features ($\gamma = 200$ mJ/mol K^2) induced by strong electronic correlations [2]. This is the third transuranium based intermetallic compound presenting superconductivity after $PuCoGa_5$ [3] and $PuRhGa_5$ [4]. These systems have relatively high critical temperature $T_c \approx 18.6$ and 9 K, respectively. Their neptunium counterparts $NpCoGa_5$ [5] and $NpRhGa_5$ [6] are not superconductors but antiferromagnets at 47 and 36 K, respectively. Taking into account the specificity of the intrinsic properties of the plutonium probably at the origin of superconductivity in the $PuTGa_5$ family, we decided to synthesize the plutonium counterpart of the $NpPd_5Al_2$, namely $PuPd_5Al_2$.

The compound of our interest was studied by means of X-ray diffraction, magnetization, specific heat and electrical resistivity performed in a wide temperature and magnetic field range (2–300 K, 0–14 T). Preliminary results have been already published elsewhere [7] but here we will focus more on structural and phase aspects (together with preparation and characterization) as well as we present some results of magnetization, specific heat and electrical resistivity of $PuPd_5Al_2$. It appears that the $ZrNi_2Al_5$-structure supports easily the actinide atom and compounds such as $ThPd_5Al_2$ [7], UPd_5Al_2 [8,9] and $CePd_5Al_2$ [10,11] have already been reported in addition to $NpPd_5Al_2$ [1,2,12]. UPd_5Al_2 is relatively difficult to obtain a pure phase and seems to do not form by flux [8]. It was then important to examine the quality of the material obtained by arc melting by several techniques (powder and single crystal X-ray diffraction, scanning electron microscopy). This is particulary challenging in the case of plutonium based materials where radioactivity and self disintegration play an important role. Here, the self-heating effect arising from the radioactive decay of the ^{239}Pu isotope ($W = 1.9$ mW/g) prevented measurements below 2 K even in the case of a very small amount of compound (<1 mg).

2. Preparation and characterization

The polycrystalline samples of $PuPd_5Al_2$ were prepared by arc melting the stoichiometric amounts of the pure metals components in the ratio Pu:1 Pd:5 Al:2. Starting materials were used in the form of 4 N Pd pellet and 5 N Al wire as supplied by A.D. Mackay Inc. and 3 N Pu metal (^{239}Pu isotope). The arc melting was performed under a high purity argon atmosphere on a water-cooled copper hearth, using a Zr alloy as an oxygen/nitrogen getter. The arc melted buttons were turned over and melted three times in order to ensure homogeneity. The weight losses after melting were smaller than 0.2%. Then the samples were examined by X-ray single crystal, powder diffraction methods and scanning electronic microscopy before physical properties examination.

The powder X-ray diffraction was done using a Bruker D8 diffractometer with the monochromated Cu$K\alpha_1$ radiation ($\lambda = 1.54059$ Å) equipped with a Vantec detector covering 6° in 2θ. The powder diffraction pattern of $PuPd_5Al_2$ is presented on Fig. 1(a). The powder patterns were recorded in the 2θ range of 15–120° (step size of 0.007°), with an exposure of 14 s per step. The diffraction patterns were analyzed by a Rietveld-type profile refinement method [13] using the WinplotR–Fullprof program [14]. The samples were mounted on a rotating device to avoid any preferential orientation effect.

Single crystals suitable for crystal structure determination were mechanically extracted from the button and mounted in a capillary

* Corresponding author. Tel.: +49 7247 951 428; fax: +49 7247 951 99 428.
E-mail address: jean-christophe.griveau@ec.europa.eu (J.-C. Griveau).

0022-3115/$ - see front matter © 2008 Published by Elsevier B.V.
doi:10.1016/j.jnucmat.2008.10.034

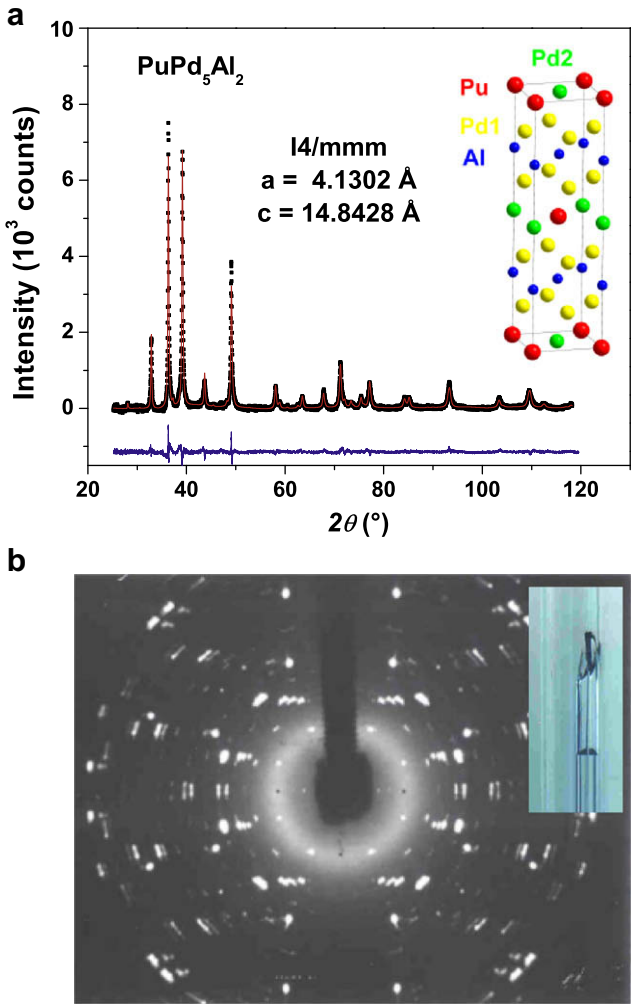

Fig. 1. (a) X-ray powder diffraction pattern ($\lambda = 1.54059$ Å) recorded for $PuPd_5Al_2$(DRX). The solid red line through experimental points is the Rietveld refinement profile calculated for tetragonal $PuPd_5Al_2$. The blue lower curve represents the difference between experimental and model results. A sketch of the crystallographic structure is presented in the inset top left. (b) X-ray single crystal diffraction pattern obtained by rotating a single crystal extracted from the batch (inset top right). (For interpretation of the references to colour in this figure legend, the reader is referred to the web version of this article).

for X-ray diffraction by rotation (Fig. 1(b)). They were examined on a Enraf–Nonius CAD-4 diffractometer with the graphite monochromatized MoK_α-radiation. The lattice constants, determined from least square analysis of the setting angles of 25 X-ray reflections, confirmed the tetragonal unit cell and are similar to those determined by X-ray powder diffraction. The crystal structure was solved by the direct method using SHELX97 [15] and the data processing using the WinGX package [16] are reported in Table 1. The crystal structure (Inset of Fig. 1(a)) was refined from the single crystal X-ray data and was corrected for Lorentz and polarization effects. It appears to be, like $NpPd_5Al_2$ [1], tetragonal with the $ZrNi_2Al_5$-type (space group $I4/mmm$) with lattice parameters $a = 4.1302$ Å and $c = 14.8428$ Å. The atomic coordinates obtained are presented in Table 2. Finally, the phase composition was determined by energy-dispersive X-ray (EDX) analysis. The measurements were performed on a Philips XL40 scanning electron microscope (SEM). The microprobe analysis (see Fig. 2) indicates that the prepared and studied samples of $PuPd_5Al_2$ were homogeneous and single phase.

Table 1
Crystallographic data for $PuPd_5Al_2$ obtained from a single crystal.

Composition	$^{239}PuPd_5Al_2$
Space group	$I4/mmm$ (No. 139)
Lattice parameters (Å)	$a = 4.1302(14)$
	$c = 14.8428(46)$
Cell volume (Å^3)	253.20
Formula units per cell	$Z = 2$
Formula mass	825.11
Calculated density (g/cm^3)	10.82
Crystal size (mm^3)	$0.03 \times 0.20 \times 0.05$
Radiation	MoK_α ($\lambda = 0.71073$ Å)
Scans up to 2θ	60°
Linear absorption coefficient	30.38 mm^{-1}
Total number of reflections	1008
	Unique: 140 ($R_F = 0.092$)
Reflections with $F_o > 4\sigma(F_o)$	81
Goodness of fit	1.040
Conventional residual R	0.0896 ($F > 4\sigma$)

Table 2
Crystallographic parameters for $PuPd_5Al_2$.

Atom	Site	x	y	z	U_{eq}
Pu	2a	0	0	0	0.0082
Pd1	8g	0.5	0	0.1456(3)	0.0063
Pd2	2b	0.5	0.5	0	0.0044
Al	4e	0	0	0.2521(20)	0.0156

The structure was refined with anisotropic displacement parameters for all atoms. The last column contains the equivalent isotropic U values (Å^2).

3. Magnetic properties

The magnetic properties were studied using a Quantum Design (QD) MPMS–7 device in the temperature range 2–300 K and in magnetic fields up to 7 T. The sample selected is presented in the inset of Fig. 3 with encapsulation. The temperature dependence of the magnetic susceptibility of $PuPd_5Al_2$ is shown on Fig. 3. The distinct maximum on $\chi(T)$ curve refers to the antiferromagnetic ordering at 5.6 K. Above 10 K the magnetic susceptibility follows a modified Curie–Weiss law with an effective magnetic moment $\mu_{eff} = 1.05\ \mu_B$, a paramagnetic Curie temperature $\Theta_p = -12.5$ K and $\chi_0 = 6.9 \times 10^{-4}$ emu/mol. The obtained value of μ_{eff} is close to 1.01 μ_B as anticipated for Pu^{3+} in the intermediate coupling configuration. The negative sign of Θ_p refers to antiferromagnetic exchange interactions and it is consistent with the antiferromagnetic ordering in the compound studied.

As shown in the upper inset of Fig. 3, a distinct peak in $\chi(T)$ is clearly observed. With increasing magnetic field the maximum in the magnetic susceptibility gradually weakens.

4. Physical properties at low-temperature

4.1. Specific heat

Heat capacity experiments were performed in the temperature range 2.5–300 K and in magnetic fields up to 14 T on a QD PPMS–14 setup using the relaxation method. The low-temperature dependence of the specific heat of a small polycrystal of $PuPd_5Al_2$ is shown in Fig. 4. Due to contamination risk the sample was encapsulated by Stycast© 2850 FT glue (sample mass = 1.44 mg, Stycast mass = 0.381 mg) [17]. Inset in Fig. 4 displays an encapsulated sample mounted on the calorimeter. A distinct λ-shaped anomaly at $T_N = 5.6$ K confirms the magnetic order in this material. When applying magnetic field the peak gradually weakens and shifts to lower temperatures (see Fig. 4). As shown in the previous

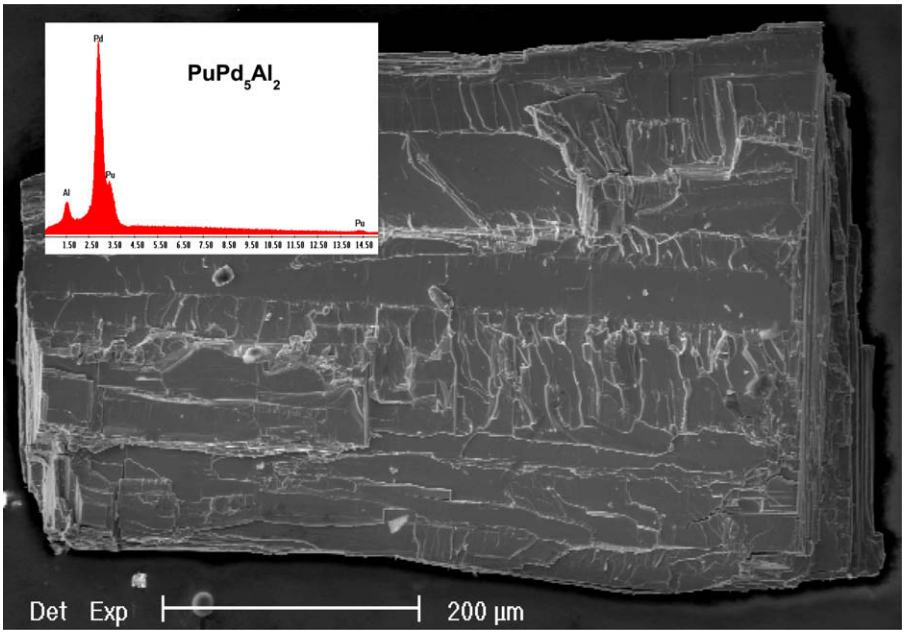

Fig. 2. SEM micrograph and EDX spectra for Pu, Pd and Al distribution contents into a sample extracted from the arc melting showing that samples are clearly homogeneous.

paper [7] the low-temperature part of the specific heat (below magnetic ordering) may be well described by a simple model that takes into account the presence of antiferromagnetic spin waves with a gap Δ in the spectrum of magnons. Within this analysis the spin-wave gap was estimated to be about 4 K [7].

4.2. Electrical resistivity

The electrical resistivity was measured from 2 to 300 K by a QD PPMS–9 device by four-probe DC technique. With decreasing temperature the electrical resistivity decreases down to the magnetic ordering temperature, whereas just below T_N the resistivity exhibits a distinct hump with a maximum at 5 K (inset of Fig. 4). The ordering temperature is 5.6 K and agrees very well with magnetic and specific heat studies. The increase of the electrical resistivity below T_N might be associated to the formation of a new "magnetic" Brillouin zone boundary in the ordered state. An other explanation might be the presence of a small gap on a part of the Fermi surface due to the formation of a spin–density–wave state [7].

4.3. Transport anisotropy

We selected two samples (*A* and *B*) extracted from the polycrystalline batch of $PuPd_5Al_2$. Sample *A* presented a needle shape while sample *B* was relatively flat displaying grains perpendicular to the main direction. The Fig. 5(a) presents the resistivity curves obtained for these two samples. The electrical current *I* was applied along the main directions for each sample. Then current *I* was parallel to grains for sample A and perpendicular to grains for sample *B*.

Here it is interesting to compare $PuPd_5Al_2$ to a recently discovered Kondo-lattice system based on Cerium, namely $CePd_5Al_2$ [10].

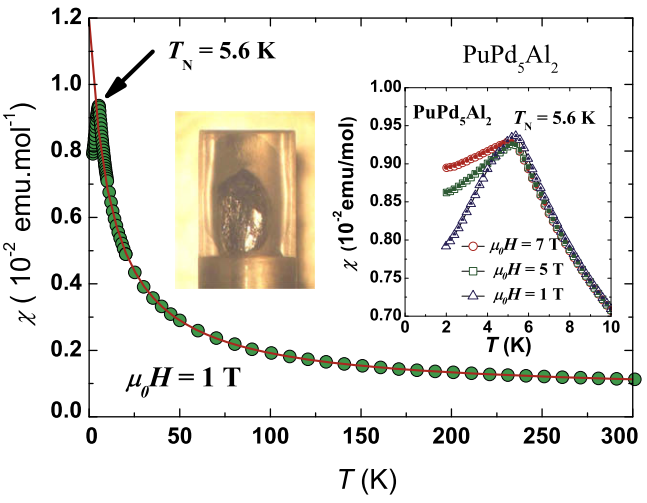

Fig. 3. Temperature dependence of the magnetic susceptibility of $PuPd_5Al_2$. The solid line is a modified Curie–Weiss fit. Lower inset: low-temperature susceptibility measured in several magnetic fields. A picture of the measured sample is presented with encapsulation.

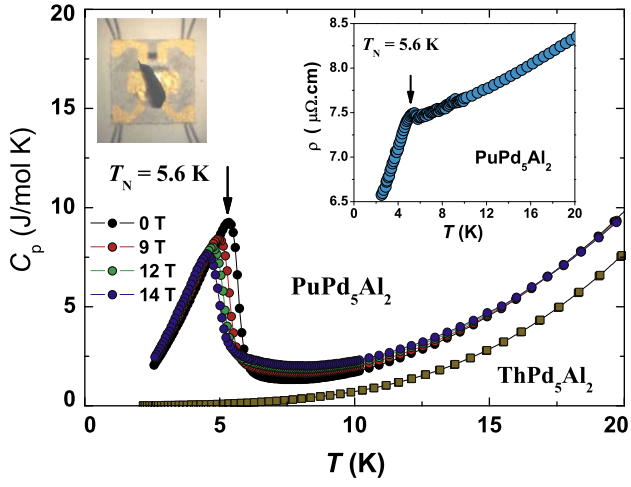

Fig. 4. Temperature dependence of the specific heat of $PuPd_5Al_2$ measured in several magnetic fields. The measured sample is displayed on the top left of the figure. The inset shows the temperature temperature dependence of the resistivity of $PuPd_5Al_2$. The magnetic ordering manifest as a peak at T_N before the decrease of the resistivity at low-temperature.

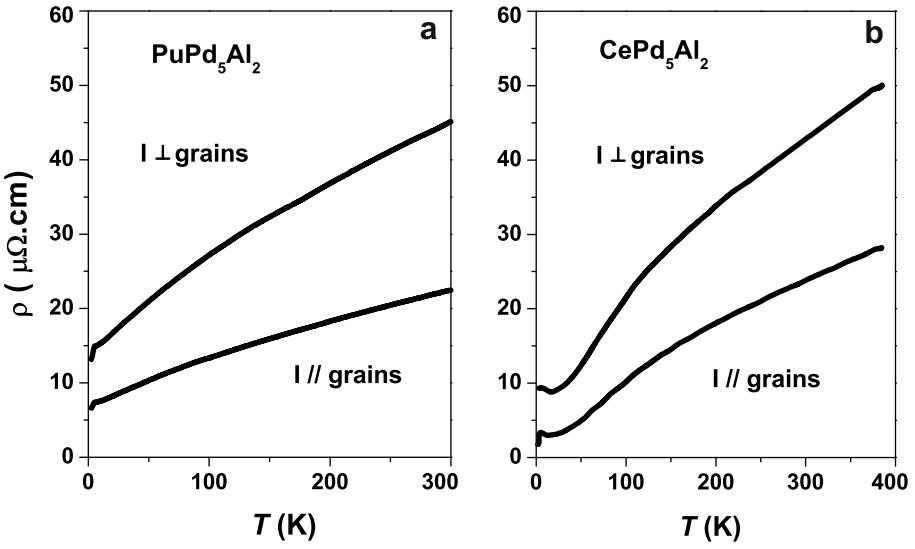

Fig. 5. (a) Temperature dependence of the electrical resistivity performed on two samples of $PuPd_5Al_2$ with different shapes and grain orientation. Sample *A* (I// grains) – presents the lower resistivity values while sample *B* (I ⊥ grains) displays a higher resistivity. (b) Temperature dependence of the electrical resistivity obtained for $CePd_5Al_2$ [10] along the main directions. The two materials present similar transport properties.

This system crystallizes in the same tetragonal structure with the $ZrNi_2Al_5$-type. It is reported as an antiferromagnetic Kondo-lattice with two magnetic transitions ($T_{N_1} \sim 3.9\,K$ and $T_{N_2} \sim 2.9\,K$) and an enhanced Sommerfeld coefficient $\gamma_e \sim 60\,\mathrm{mJ/mol\,K^2}$. The Fig. 5(b) presents the resistivity curves obtained for the electrical current *J* applied along the main directions of single crystals of $CePd_5Al_2$. They present strong similarities (shape and values). Moreover, their magnetic and specific heat are also very close in overall shape and value. One last important point is that $CePd_5Al_2$ becomes a superconductor at $T_c \sim 0.57$ K under pressure (9–10 GPa [11]). This aspect suggests the possibility that $PuPd_5Al_2$ may become superconductor at a moderate pressure range.

5. Summary

A compound $PuPd_5Al_2$ was synthesized, characterized and studied in a wide temperature and magnetic field range. The compound crystallizes, like $NpPd_5Al_2$, in the tetragonal unit cell of $ZrNi_2Al_5$-type. All the results obtained indicate that, while $NpPd_5Al_2$ is a heavy-fermion superconductor at 4.9 K, $PuPd_5Al_2$ orders antiferromagnetically below 5.6 K and does not present any hint of superconductivity down to 2 K. Strong similarities exist between $PuPd_5Al_2$ and $CePd_5Al_2$, the latter becoming superconductor under pressure.

Acknowledgements

We thank D. Bouëxière and H. Thiele for technical assistance. High purity Pu metal was made available through a loan agreement between Lawrence Livermore National Laboratory and ITU, in the frame of a collaboration involving LLNL, Los Alamos National Laboratory and the U.S. Department of Energy. K. Gofryk acknowledges the European Commission for support in the frame of the 'Training and Mobility of Researchers' programme.

References

[1] D. Aoki, Y. Haga, T.D. Matsuda, N. Tateiwa, S. Ikeda, Y. Homma, H. Sakai, Y. Shiokawa, E. Yamamoto, A. Nakamura, R. Settai, Y. Ōnuki, J. Phys. Soc. Jpn. 76 (2007) 063701.
[2] J.-C. Griveau, K. Gofryk, J. Rebizant, Phys. Rev. B 77 (2008) 212502.
[3] J.L. Sarrao, L.A. Morales, J.D. Thompson, B.L. Scott, G.R. Stewart, F. Wastin, J. Rebizant, P. Boulet, E. Colineau, G.H. Lander, Nature 420 (2002) 297.
[4] F. Wastin, P. Boulet, J. Rebizant, E. Colineau, G.H. Lander, J. Phys.: Condens. Matter 15 (2003) 2279.
[5] E. Colineau, P. Javorský, P. Boulet, F. Wastin, J.-C. Griveau, J. Rebizant, J.P. Sanchez, G.R. Stewart, Phys. Rev. B 69 (2004) 184411.
[6] E. Colineau, F. Wastin, P. Boulet, P. Javorský, J. Rebizant, J.P. Sanchez, J. Alloy. Compd. 386 (2005) 57.
[7] K. Gofryk, J.-C. Griveau, E. Colineau, J. Rebizant, Phys. Rev. B 77 (2008) 092405.
[8] Y. Haga, D. Aoki, Y. Homma, S. Ikeda, T.D. Matsuda, E. Yamamoto, H. Sakai, N. Tateiwa, N.D. Dung, A. Nakamura, Y. Shiokawa, Y. Onuki, J. Alloy. Compd. 464 (2008) 47.
[9] Y. Haga, T.D. Matsuda, S. Ikeda, E. Yamamoto, N. Duc Dung, Y. Onuki, J. Phys. Soc. Jpn. 77 (Suppl. A) (2008) 365.
[10] R. de A. Ribeiro, T. Onimaru, K. Umeo, M. de A. Avila, K. Shigetoh, T. Takabatake, J. Phys. Soc. Jpn. 76 (2007) 123710.
[11] F. Honda, M.-A. Measson, Y. Nakano, N. Yoshitani, E. Yamamoto, Y. Haga, T. Takeuchi, H. Yamagami, K. Shimizu, R. Settai, Y. Onuki, J. Phys. Soc. Jpn. 77 (2008) 043701.
[12] D. Aoki, Y. Haga, T.D. Matsuda, N. Tateiwa, S. Ikeda, Y. Homma, H. Sakai, Y. Shiokawa, E. Yamamoto, A. Nakamura, R. Settai, Y. Onuki, J. Phys. Soc. Jpn. 77 (Suppl. A) (2008) 159.
[13] T. Roisnel, J. Rodriguez-Carvajal, Mater. Sci. Forum 378 (2001) 118.
[14] H.M. Rietveld, J. Appl. Crystallogr. 2 (1969) 65.
[15] G.M. Sheldrix, SHELX-97, Universität Göttingen, 1997.
[16] L.J. Farrugia, J. Appl. Crystallogr. 32 (1999) 837.
[17] P. Javorský, F. Wastin, E. Colineau, J. Rebizant, P. Boulet, G.R. Stewart, J. Nucl. Mater. 344 (2005) 50.